NACA

RESEARCH MEMORANDUM

AN INVESTIGATION OF SINGLE-DEGREE-OF-FREEDOM SNAKING

OSCILLATIONS ON A MODEL OF A HIGH-SPEED RESEARCH

AIRPLANE BY THE NACA WING-FLOW METHOD

By Harold I. Johnson and Stanley Faber

Langley Aeronautical Laboratory
Langley Field, Va.

CLASSIFICATION CHANGED

UNCLASSIFIED

By authority of _____ NACA Res abs _____ Date _____ June 24, 1956 _____

_____ IRA-128 _____

Abul 8 21-58

FOR REFERENCE

NOT TO BE TAKEN FROM THIS ROOM

NATIONAL ADVISORY COMMITTEE
FOR AERONAUTICS

WASHINGTON
August 7, 1951

NATIONAL ADVISORY COMMITTEE FOR AERONAUTICS

RESEARCH MEMORANDUM

AN INVESTIGATION OF SINGLE-DEGREE-OF-FREEDOM SNAKING

OSCILLATIONS ON A MODEL OF A HIGH-SPEED RESEARCH

AIRPLANE BY THE NACA WING-FLOW METHOD

By Harold I. Johnson and Stanley Faber

SUMMARY

An investigation was made by the wing-flow method to determine the snaking characteristics of a $\frac{1}{40}$-scale partial-model of a research airplane. In addition, the snaking characteristics of 11 modified configurations of the research-airplane model were determined as well as the characteristics of another model that had greater fineness ratios. The basic models had a fuselage and a vertical tail and were mounted on the wing-flow test panel with freedom to rotate in yaw only.

Results of the tests showed that the research-airplane model in the original configuration had a snaking oscillation of appreciable amplitude at subsonic speeds. The tests showed that snaking can be caused by flow separation. In the subject investigation the flow separation and consequent snaking were largely eliminated by reducing the rates of closure of the bodies and aerodynamic surfaces to small values.

INTRODUCTION

Flight tests of several high-speed airplanes of the research and tactical types have shown that short-period small-amplitude lateral-directional oscillations, commonly called snaking, exist. Finding the cause and cure for these oscillations is of primary importance because these oscillations reduce the value of an airplane as a gun platform or as a vehicle for directing accurately either self-propelled missiles or freely-falling bombs. In the commercial airplane these oscillations would reduce the comfort and desirability of flight.

Past attempts to explain snaking with the aid of classical lateral-stability theory employing three degrees of freedom have met with little success. Usually it is found that the large-amplitude Dutch roll oscillations damp approximately in accordance with calculation but that the small-amplitude snaking oscillations persist despite calculated indications to the contrary. These results suggest that snaking may not be connected intimately with classical lateral-stability theory but may be caused by other phenomena which are not considered in the theory. One possibility is that snaking may be simply a small forced oscillation arising from flow separation, boundary-layer instability, or some other discrete forcing function. Another possibility is that snaking is a small unstable oscillation arising from a phase shift between motions of the airplane and changes in the boundary-layer flow pattern. If either possibility be true, then one would expect a snaking oscillation to be possible even though an airplane or model is restricted to one-degree-of-freedom motion in yaw.

In order to investigate this particular phase of the snaking problem, a series of tests were made on a $\frac{1}{40}$-scale model of a high-speed research airplane by utilizing the wing-flow technique. The basic model consisted only of the fuselage and vertical tail of the research airplane and was mounted on the wing-flow test panel by means of an elastic pivot which allowed the model freedom to rotate in yaw only. Various modifications were made to the fuselage and vertical tail of the model to determine their effect on the snaking characteristics.

This paper presents reproductions of actual flight records showing the snaking behavior of the various model configurations as they were carried through a Mach number range from 0.70 to 1.15. On the basis of the results from these tests, a second model with a much thinner vertical tail and a more slender fuselage was designed and tested. This model was expected to be relatively free from snaking tendencies.

MODELS AND APPARATUS

The basic model investigated was a $\frac{1}{40}$-scale model of the top half of the fuselage and the complete vertical tail of a high-speed research airplane. A drawing of the model is given in figure 1. It will be noted that the model was provided with a cylindrical-mounting tang through the design center-of-gravity position at 59.2 percent of the body length. This tang passed through the upper surface of the wing-flow test panel and was attached to an instrument having an elastic pivot that allowed the model freedom to rotate in yaw only. A view of the model mounted on the wing-flow airplane is given in figure 2 and a close-up photograph of

the basic model is shown in figure 3. The model was constructed primarily from solid mahogany and had a polished lacquer finish.

The fuselage in plan view had a rather abrupt rate of closure near the rear end; the total included angle between tangents to the fuselage sides at the point of termination of the fuselage was 38°. Hereinafter this angle is referred to as the fuselage trailing-edge angle. The vertical tail had NACA 27-010 and NACA 27-008 airfoil sections at the root and tip, respectively. These sections gave the vertical tail an average trailing-edge angle of 20°.

In order to insure that the top half of the model fuselage was completely clear of the boundary layer over the wing-flow test panel, the fuselage was deepened by $\frac{1}{4}$ inch. This increase in fuselage depth would also tend to make the directional stability of the model fuselage more nearly equal to that of the complete research-airplane fuselage. The model was provided with an 0.032-inch-thick end plate, the bottom of which was $\frac{1}{16}$ inch above the wing-flow test panel. The purpose of this end plate was to simulate semimodel test conditions. It is not known what effect the juncture of the end plate and fuselage might have had in promoting flow separation.

Several modifications were made to the basic configuration during the test program including changes to the shape of the rearward portions of the fuselage and vertical tail, addition of the horizontal tail, addition of a sidewash-generating vane, and addition of transition and separation wires. These modifications are described briefly in table I and further details are given in a subsequent section of the paper. The term "slab" is used in this paper to define a fuselage or vertical-tail configuration for which the rearmost cross section is the same as the corresponding maximum cross section. Figures 4 and 5 show two of the main modifications investigated.

In order to gain some idea of the smallest-amplitude oscillations that could be expected with any model mounted on the F-51D wing-flow test panel, a second model was designed and tested. This model is shown in figures 6 and 7. The fuselage consisted of a half-body of revolution formed from an NACA 65A006 airfoil section to which a pointed nose had been added. The use of this airfoil section resulted in a body having an included trailing-edge angle of only 6.5°. The fuselage had the same length and pivot-axis location as the research-airplane model and was also deepened by $\frac{1}{4}$ inch as in the case of the airplane model. The vertical tail had the same plan form as that on the airplane model but was much thinner; the root thickness ratio was only 0.7 percent chord and the tip thickness ratio was only 2.9 percent chord. Furthermore, the

vertical-tail section was formed from a flat steel plate by simply
sharpening the leading edge so that the trailing-edge angle was main-
tained at 0°. Inasmuch as this model was characterized by very high
fineness ratios and negligibly small trailing-edge angles, it was thought
that the model would be sensibly free from any snaking tendencies due to
flow separation; consequently, the oscillations of this model might be
construed to represent the degree of fluctuation inherent in the flow
over the wing-flow test panel and/or the amplitude of any oscillations
arising from possible structural vibrations of the wing-flow test air-
plane.

The moments of inertia of the two models about the pivot axis were
determined experimentally as 0.000626 slug-feet^2 for the original research-
airplane model with vertical tail only and 0.000314 slug-feet^2 for the
high-fineness-ratio model. Modifications made to the research-airplane
model increased its moment of inertia by only small undetermined amounts.

The models were attached rigidly to the shaft of a control-position-
recording instrument (see fig. 5) and were carefully mass-balanced about
the axis of the shaft. The shaft of the control-position recorder was
supported by two sets of flexible crossed springs made from flat Swedish
blue steel. This arrangment gave a model-support bearing that had
vanishingly small static friction, zero play, and substantially infinite
stiffness in all directions except for rotation of the models in yaw.
Of course, the bearing had an inherent restoring force in yaw which would
be expected to affect the nature of any free model oscillation; however,
the spring constant was purposely kept as low as possible so as to make
the effect of the spring support on the model oscillations as small as
possible. That this aim was achieved is indicated by the fact that, in
flight, the lowest oscillation frequency recorded was about 12 cycles
per second whereas, on the ground, the frequency of a free model oscil-
lation was only 2.8 cycles per second. Because the restoring moment
varies as the square of the frequency ratio, these figures indicate the
spring restoring forces were negligibly small compared to the aerodynamic
restoring forces; consequently, the oscillation characteristics measured
in flight were almost wholly determined by the aerodynamic phenomena.
The damping of the model-support system was also extremely small. A free
oscillation of 5° initial amplitude on the ground in still air was easily
visible after 5 minutes so that, when the air damping in this case is
considered, it must be concluded that the mechanical damping inherent in
the instrument was vanishingly small.

The control-position recorder (fig. 5) employed an optical recording
system in which a focussed light beam is reflected from a small mirror
at the bottom of the movable support onto a continuously moving strip of
film. On the same strip of film a trace was obtained from a solenoid-
actuated 0.1-second timer. By this means a continuous record, without
lag, of the position of the model was obtained.

TESTS

The test procedure consisted simply of diving the wing-flow airplane through its permissible speed range starting from an altitude of 28,000 feet and making a 4g pull-out at an altitude of approximately 18,000 feet. The resulting model Mach number range was from approximately 0.70 to 1.15. Continuous records were obtained of the model position. In a few runs tuft surveys of the flow conditions on the model were also made using a 16-millimeter gun camera with telephoto lens mounted in the airplane fuselage. For the tuft surveys, fine thread tufts were glued to the fuselage and vertical tail of the model as shown in figure 3. Continuous records also were obtained of the position of a rectangular free-floating vane located $22\frac{1}{2}$ inches outboard of the model (fig. 2). These records were examined to ascertain the air-flow steadiness associated with atmospheric turbulence. Only runs made in relatively smooth air were used. No attempt was made to measure high-frequency disturbances with the rectangular free-floating vane.

The Mach numbers given in this paper were arbitrarily chosen as those that would have been measured with model removed by a flush-type orifice in the wing-flow panel located at 70 percent of the body length. Typical variations of local Mach number with chordwise position for the test panel are presented in figure 8. The Mach number decreases with vertical distance above the panel by about 0.7 percent per inch height. A plot of the Reynolds number of the tests based on body length is also included in figure 8.

RESULTS AND DISCUSSION

Figure 9 contains reproductions of the actual flight records from the model position recording instrument for all the configurations tested. The first four records (configurations A, B, C, and D) show the effects of changes in shape of the fuselage with the original vertical tail in place. The next three records (configurations E, F, and G) also show fuselage-shape effects but with the full-slab vertical tail in place. A cross comparison of these two groups, configuration A with E, B with F, and D with G shows the effect of making the vertical tail flat rearward of the line of maximum thickness. The effect of the presence of the horizontal tail can be seen by comparing configurations A with H and B with I. The effect of a separation wire wrapped around the fuselage at 84 percent of the body length can be seen by comparing configurations E and J. The effect of a boundary-layer transition wire wrapped around the fuselage at 21.9 percent of the body length is seen by comparing

configurations E and K. The effects of a sidewash-generating vane
located near the center of gravity are found by comparing configurations
A and L. The bottom record on figure 9 is that obtained with the high-
fineness-ratio model. All the records on figure 9 are alined vertically
at M = 1.0 and a time scale is shown at the bottom.

Original model (configuration A).- The original model had a ±0.5°

snaking oscillation at speeds up to a Mach number of 0.85. Between Mach
numbers of 0.85 and 0.97 the amplitude of the oscillation increased
markedly and reached ±1.5° at a Mach number of 0.91. From Mach numbers
of 0.97 to 1.15 the oscillations were much smaller (amplitude ±0.25°)
except for a narrow band at a Mach number of 1.13. The amplitude of the
oscillations was not constant but continually increased and decreased in
much the same manner as has been observed for snaking oscillations of some
full-scale airplanes.

The frequency of the snaking oscillations was found to be determined
by the directional stability of the model and the model moment of inertia
about the Z-axis. This conclusion resulted from calculations of frequenc
based on preliminary flight test work in which the directional stability
of the model was estimated from the change in floating angle caused by a
constant applied yawing moment, and the model moment of inertia was deter
mined experimentally.

A comparison between these calculated frequencies and measured fre-
quencies taken from the oscillation record of configuration A is given
in the following table:

Mach number	Experimental frequency (cps)	Calculated frequency (cps)
0.70	13.5	13.5
.75	15.0	15.5
.80	17.0	15.4
.85	17.0	15.4
.90	16.0	15.4
.95	15.1	17.2
1.00	20.2	17.6
1.05	21.5	18.2
1.10	21.5	19.3

These model oscillations correspond to the normal short-period lateral-
directional oscillations of a full-size airplane; however, for the
full-size airplane the period would be much longer because of the increase
in size and would be modified somewhat because of the additional degrees
of freedom in roll and lateral translation.

Effect of fuselage shape (configurations A, B, C, and D; configu-
rations E, F, and G).- The first possibility investigated was that the
snaking oscillations were caused by flow unsteadiness generated in the
wake at the blunt rear end of the body and transmitted forward to the
sides of the fuselage through the boundary layer. Accordingly, in an
attempt to reduce or possibly eliminate the turbulent wake at the end
of the fuselage, the blunt end was eliminated by adding a balsa-wood
cone to the end of the fuselage (configurations B and F). This theory
proved to be totally incorrect as can be seen from figure 9. The snaking
oscillations increased in amplitude by a factor of about 3 at subsonic
speeds and were substantially unchanged at supersonic speeds. These
results led to the tentative conclusion that initial flow separation was
occurring slightly forward of the fuselage end; in this case, the
increased amplitude of the oscillations caused by the cone fairing could
be explained by the fact that the cone added additional fuselage side
area in a region of unsteady separated flow. Therefore, the magnitude
of the unsteady impulses on the fuselage was increased.

If this theory was assumed to be correct, the next logical step
appeared to be to reduce the rate of closure (decrease the trailing-edge
angle) of the fuselage. This step would have the effect of reducing
the rate-of-pressure recovery near the end of the fuselage and might
therefore reduce or eliminate separation off the sides of the fuselage.
Consequently, configurations C and D, incorporating a semi-slab and a
full-slab fuselage, respectively, were tried. The semi-slab configu-
ration had a tail-end cross section halfway between the original tail-
end cross section and the maximum fuselage cross section. The sides of
the added pieces were straight and tangent to the original fuselage
surface at the points of contact. This modification had the effect of
reducing the fuselage included trailing-edge angle from 38° to 11.2°.
The full-slab configuration was obtained simply by maintaining the maxi-
mum fuselage cross section all the way back to the end of the fuselage.
For this case, of course, the fuselage trailing-edge angle was 0°.

The results of reducing the fuselage trailing-edge angle were very
beneficial (configurations C, D, and G). The oscillations at subsonic
speeds for the most part had an amplitude of only ±0.2°. This amplitude
is believed to be approximately the lowest amplitude of oscillation
that can be expected with any model mounted on the wing-flow test panel.
Of interest is the fact that the semi-slab fuselage was about as effec-
tive as the full-slab fuselage in reducing the amplitude of the oscil-
lations. At supersonic speeds, where the model oscillations were
already small, the fuselage modifications had no significant effects.

Effect of vertical-tail section (configurations A with E, B with F,
and D with G.- The possibility that the relatively large trailing-edge

angles ($\approx20^\circ$) on the vertical tail might be contributing to the snaking oscillations was also studied. The original vertical tail was made flat-sided behind the line of maximum thickness. This modification appeared to cause a slight but noticeable reduction in amplitude of the directional oscillations between Mach numbers of 0.95 and 1.15.

Effect of presence of horizontal tail (configurations A with H, and

B with I.- The presence of the horizontal tail had little effect on the snaking characteristics of the model with one exception. The largest amplitude oscillations that had occurred in the region Mach number approximately 0.90 were delayed to Mach number of approximately 1.00 when the horizontal tail was added. This effect is probably related to interference between the horizontal tail and the wing-flow test panel. It is realized, of course, that the addition of the horizontal tail constituted an incorrect application of the wing-flow technique inasmuch as one would expect the occurrence of choked flow beneath the horizontal tail in the transonic speed range. The results obtained, however, at the lowest test speeds may be of interest.

Effect of separation wire (configuration E with J).- In order to see if the snaking oscillation was caused primarily by alternate forward and rearward movement of the points of separation on the opposite sides of the fuselage, an 0.065-inch-diameter separation wire was wrapped around the fuselage at 84 percent of the fuselage length. This location was estimated to be somewhat forward of the point at which uncontrolled separation occurred. The idea behind the separation wire was to make the point of separation independent of yaw angle. Figure 9 shows that configuration J which incorporated the separation wire had a somewhat larger oscillation at subsonic speeds than configuration E. Although it is not known how effective the wire actually was in fixing the location of separation, it appears that the use of this particular separation-controlling device had no value as a cure for the snaking oscillations investigated.

Effect of transition wire (configuration E with K).- There was reason to suspect that, because of the highly polished model surface and the relatively low Reynolds number of the tests, the boundary layer ahead of the region of separation might be laminar. Since a laminar boundary layer is less resistant to separation than a turbulent boundary layer, an attempt was made to insure that the boundary layer would be turbulent ahead of the region of separation. Accordingly, a 0.005-inch-diameter transition wire was wrapped around the fuselage at 21.9 percent of the fuselage length (the station at which the canopy cross-section area was a maximum). A comparison between the results for configurations E and K in figure 9 shows that the snaking characteristics in the two cases were

the same. Inasmuch as the transition wire had no effect, it appears
either that the boundary layer on the original model had been turbulent
prior to the addition of the transition wire or that the wire did not
effect permanent transition to a turbulent boundary layer. There remains,
of course, the more remote possibility that the transition wire succeeded
in bringing about a change in the basic nature of the boundary layer
without measurably affecting the phenomena directly responsible for the
snaking.

Effect of sidewash vane (configuration A with L).- The thought was
advanced that perhaps the snaking oscillation could be damped considerably
by introducing a sidewash-generating vane ahead of the vertical tail.
The theory was that if a sidewash variation could be superimposed on the
normal angle of sideslip variation of the vertical tail during snaking,
and if the phase shift in the two variations was proper, some damping of
the oscillation would result. To check this theory a small triangular
vane was attached to the top of the fuselage (figs. 1 and 5) approximately
at the center of gravity of the model. The location of the vane was
fixed partly by the consideration that no appreciable change in direc-
tional stability due to direct aerodynamic forces on the vane was desired.
The size and shape of the vane was selected on the basis of considerable
static wind-tunnel tests done by personnel of the Langley stability
tunnel. A comparison between configurations A and L in figure 9 indicates
the presence of the sidewash vane was injurious to the snaking charac-
teristics in the subsonic speed range. This result may have been caused
by the possible effects of the wake shed from the sidewash vane enveloping
the vertical tail twice during each oscillation. A method for avoiding
this phenomena might be to use two sidewash vanes in a V arrangement.
Such a modification was not tested. At supersonic speeds the sidewash
vane appeared to reduce somewhat the amplitude of the small oscillations.

Characteristics of second model (configuration M).- The bottom
record on figure 9 indicates that the second model was substantially free
from snaking tendencies throughout the test speed range as had been
expected. Some small oscillations of amplitude ±0.2° occurred. These
oscillations are believed to represent the lowest amplitude oscillations
that can be expected with any model placed on the wing-flow test panel.
The oscillations are thought to be associated with structural vibrations
of the wing-flow airplane and possible minute flow-direction fluctuations
over the wing-flow test panel. It is interesting to note that the
research-airplane model with full-slab fuselage and vertical tail (con-
figuration G) had oscillation characteristics similar to those of the
second model.

Tuft observations.- Tuft surveys of configuration L were made and
one frame from the motion-picture films is reproduced in figure 10.

This picture was taken at a Mach number of 0.86 during one of the more violent snaking oscillations. Separated flow near the extreme rear end of the fuselage is indicated by the double images of the two rearmost fuselage tufts located at 98 and 94 percent of the fuselage length (refer also to fig. 3 for tuft orientation). The motion pictures showed that the rearmost tuft fluttered throughout the entire speed range although its motion was of relatively smaller amplitude at supersonic speeds. The tuft at 94 percent fuselage length fluttered only during violent oscillations of the model. From viewing the motion pictures it was apparent that movements of the tufts were much more rapid frequencywise than movements of the model.

The tuft observations and the snaking records both lend support to the theories that snaking, in many instances, may be either a small forced oscillation arising from flow separation or boundary-layer instability or a small unstable oscillation arising from coupling between motions of an airplane and changing boundary-layer flow patterns. In order to learn more about which particular phenomena is involved, further tests at larger scale are needed. These tests should include synchronized measurements of the motion of the airplane or model, the boundary layer characteristics, and surface pressure distributions. The instrumentation for such an investigation will have to be capable of defining small lags in relation to the period of the motion involved.

Interpretation of results.- Because of the relatively low Reynolds numbers of the tests, the results presented must be considered qualitative rather than quantitative until more work has been done at full scale. Recent experiences at full scale both in this country and in Great Britain, however, indicate very strongly that the phenomenon of separation and associated snaking oscillations investigated herein occurs also at flight values of Reynolds number.

General remarks.- The method used herein to reduce the snaking oscillations of the research-airplane model may not always be practical because it might possibly lead to a prohibitive increase in fuselage base-pressure drag. Actually, however, if the fuselage rate of closure is decreased only enough to eliminate separation off the sides, the total drag may not increase noticeably inasmuch as the very existence of flow separation is usually a sign that excessive drag already is present. Note again in this connection that the semi-slab fuselage configuration tested was approximately as effective in reducing the amplitude of the oscillations as the full-slab configuration. Probably a better way than that used herein to reduce separation on existing designs would be to reduce the rate of closure of the fuselage by increasing the fuselage length so as not to incur the penalty of increased base-pressure drag. The important point indicated by the investigation is that in new designs the use of fuselages with high rates of closure

should be avoided. In this connection, however, it is not known what the effect of a jet or rocket stream issuing from the rear end of the body would be on separated flow occurring on the fuselage surface slightly forward of the jet or rocket exit.

Another method that seems attractive for eliminating separated flow near the ends of bodies having large rates of closure and near the trailing edges of wings having large trailing-edge angles is boundary-layer suction applied through a porous surface. This method was not tried in the subject investigation.

CONCLUSIONS
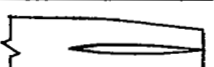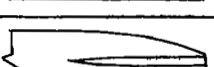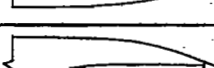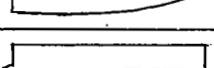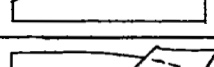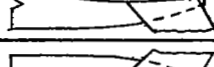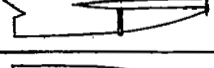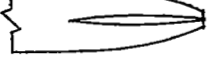
On the basis of results of a snaking investigation carried out by the wing-flow method on a $\frac{1}{40}$-scale model of a research airplane and on a second model, the following conclusions were reached:

1. The research-airplane model exhibited a one-degree-of-freedom snaking oscillation of appreciable amplitude in the subsonic speed range.

2. Snaking can be caused by local flow separation; however, local flow separation may not always be the cause of snaking.

3. In the subject tests the snaking was largely eliminated by making the rates of closure and the trailing-edge angles of the aerodynamic bodies and surfaces small.

Langley Aeronautical Laboratory
    National Advisory Committee for Aeronautics
        Langley Field, Va.

TABLE I

MODEL CONFIGURATIONS

Configuration		Fuselage	Trailing-edge angle (deg)	Tail	Trailing-edge angle (deg)	Additions
A		Original	38	Original	20	None
B		Cone added	38	Original	20	None
C		Semi-slab	11	Original	20	None
D		Full-slab	0	Original	20	None
E		Original	38	Full-slab	0	None
F		Cone added	38	Full-slab	0	None
G		Full-slab	0	Full-slab	0	None
H		Original	38	Original	20	Horizontal tail
I		Cone added	38	Original	20	Horizontal tail
J		Original	38	Full-slab	0	0.065-inch wire at $0.84l$
K		Original	38	Full-slab	0	0.005-inch at $0.22l$
L		Original	38	Original	38	Sidewash generator at center of gravity
M		Second Model	6.5	Slab-tail	0	None

Endplate -.092 Thick

3.6

3.850

BODY COORDINATES,
PERCENT LENGTH

STA	RADIUS	HEIGHT
0	0	0
4.405	1.154	1.154
8.485	2.176	2.176
17.181	—	5.542
17.621	3.912	—
21.639	4.326	6.714
27.974	4.581	6.722
34.581	4.846	6.722
45.595	5.286	6.722
73.242	5.286	6.722
84.256	4.856	5.374
86.784	4.626	4.775
91.189	4.018	4.529
95.595	2.978	4.035
100.0	1.542	3.084

Root Chord 1.315

25 % Chord

40°

11.35

2°

0.875

VERTICAL-TAIL SECTION
ROOT   27-010
TIP   27-008

Laminated Mahogany

Location of Sidewash Vane

Location of transition wire

25°

41.5°

3.0

0.988

Fuselage ℄

Baseline

Radius

Canopy faired to fuselage

Height

0.25

Baseline

Sta 2.456   Sta 8.313

3.5

6.725

Mounting Tang

Location of separation wire

.156 Radius

NACA

Figure 1.- Drawing of $\frac{1}{40}$ -scale research-airplane model. Dimensions are in inches.
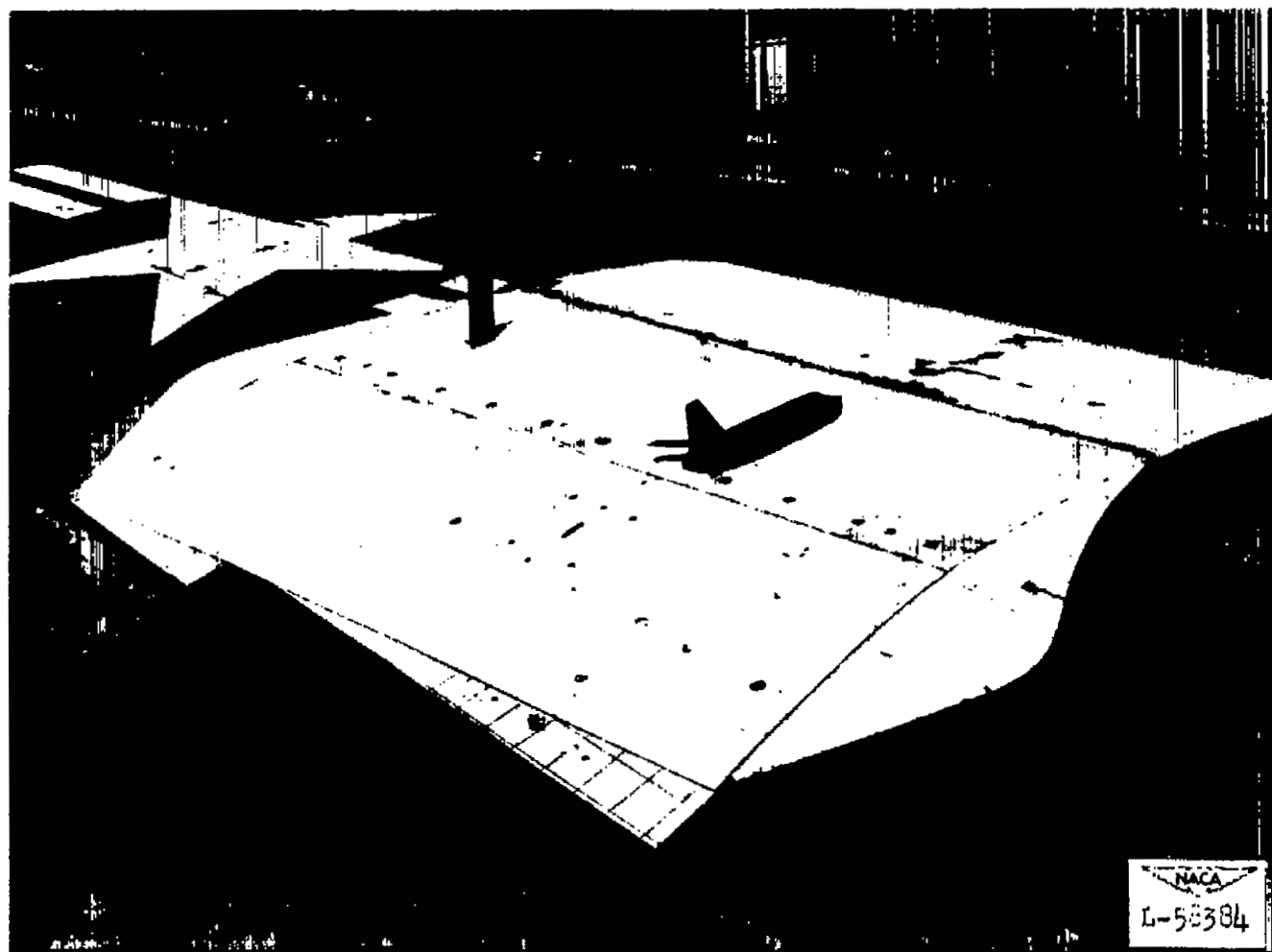
Figure 2.- Research-airplane model with horizontal tail mounted on the
wing-flow test airplane.   Rectangular vane on left used to gage
steadiness of air flow.
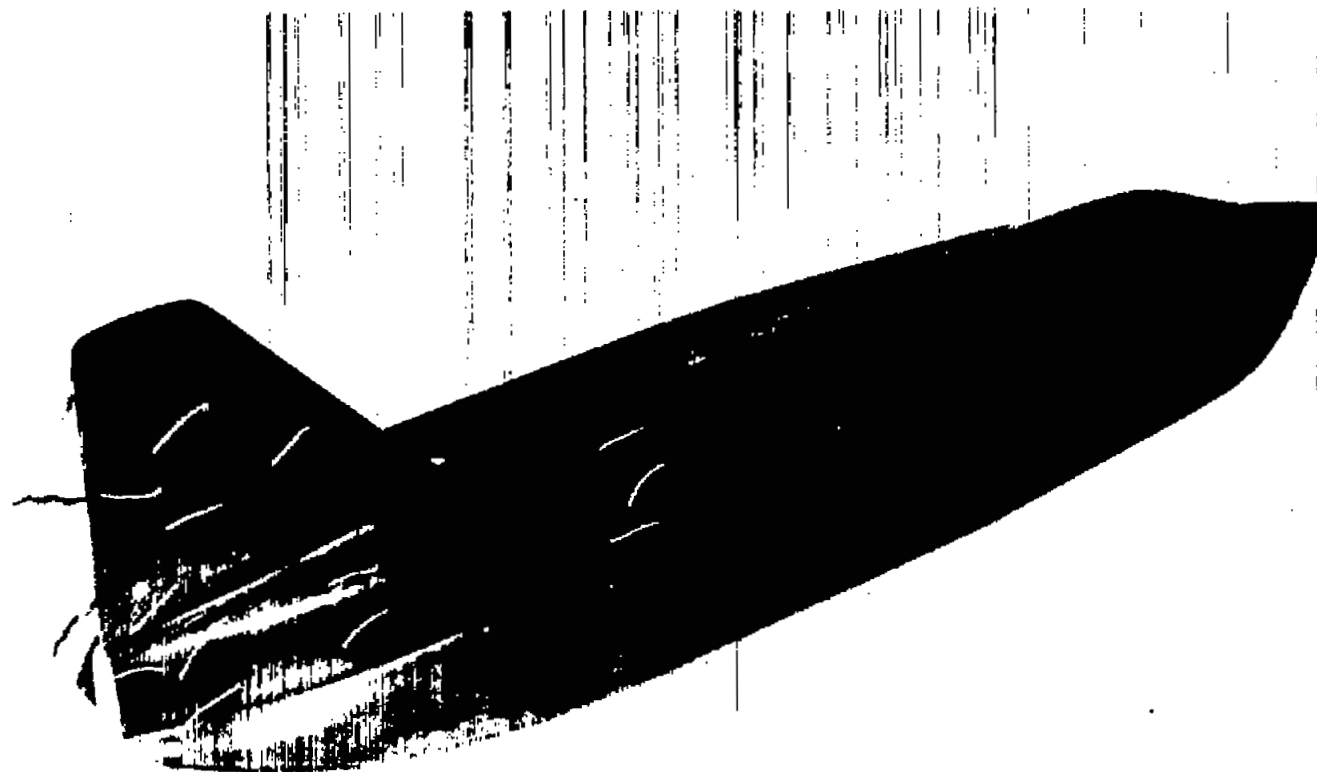
L-65952

Figure 3.- Photograph of original research-airplane model showing
locations of thread tufts.
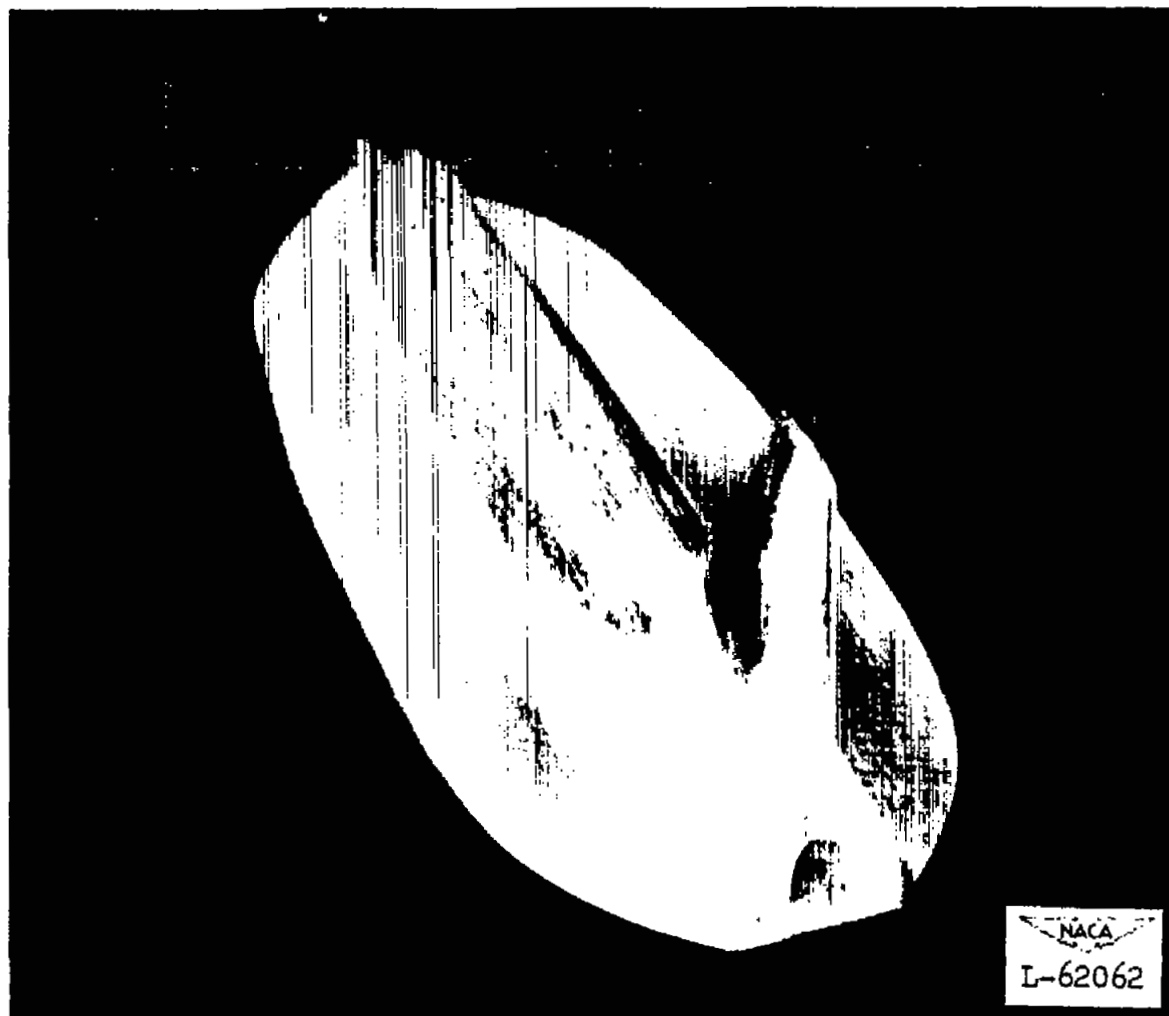
Figure 4.- Research-airplane model with full-slab fuselage and
vertical tail.
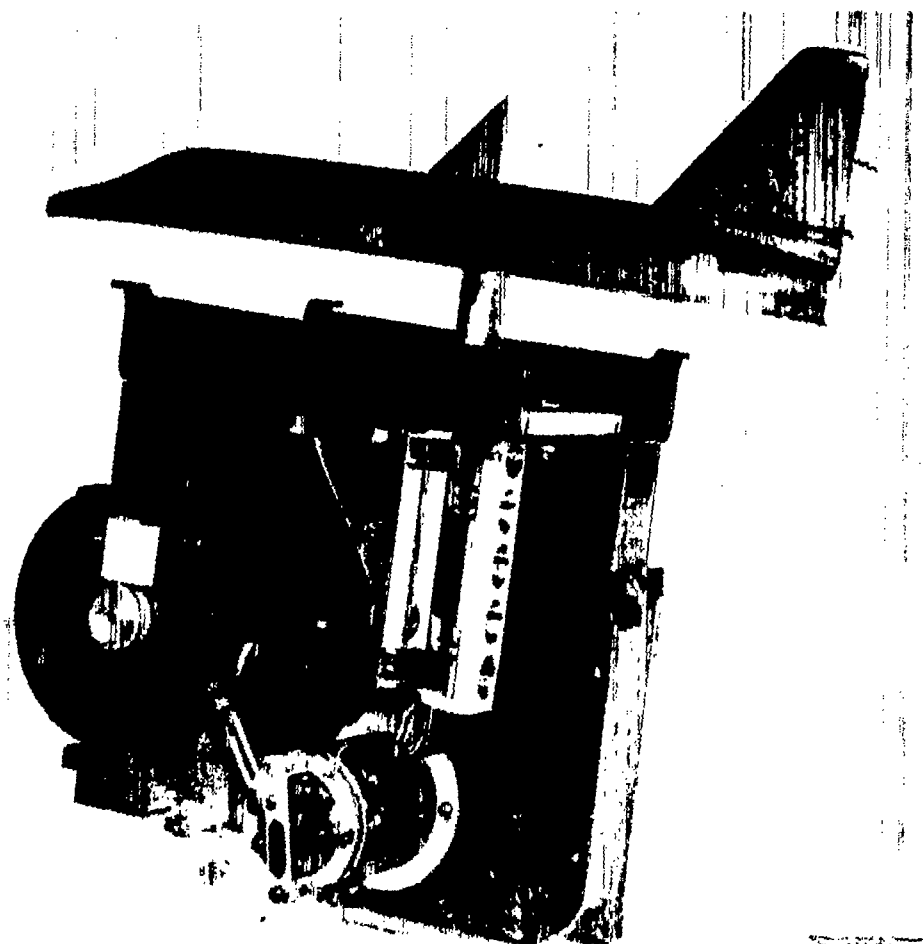
L-65095

Figure 5.- Research-airplane model mounted on position recording
    instrument. Note sidewash generator mounted on model and crossed-
    spring pivot arrangement in instrument.

Endplate   0.025 Thick

1.80

11.35

2°

0.875

0.25

0.025 Swedish
blue steel

3.0

Mahogany

0.25 Dural Plate

3.5

Mounting Tang

6.725

156 Radius
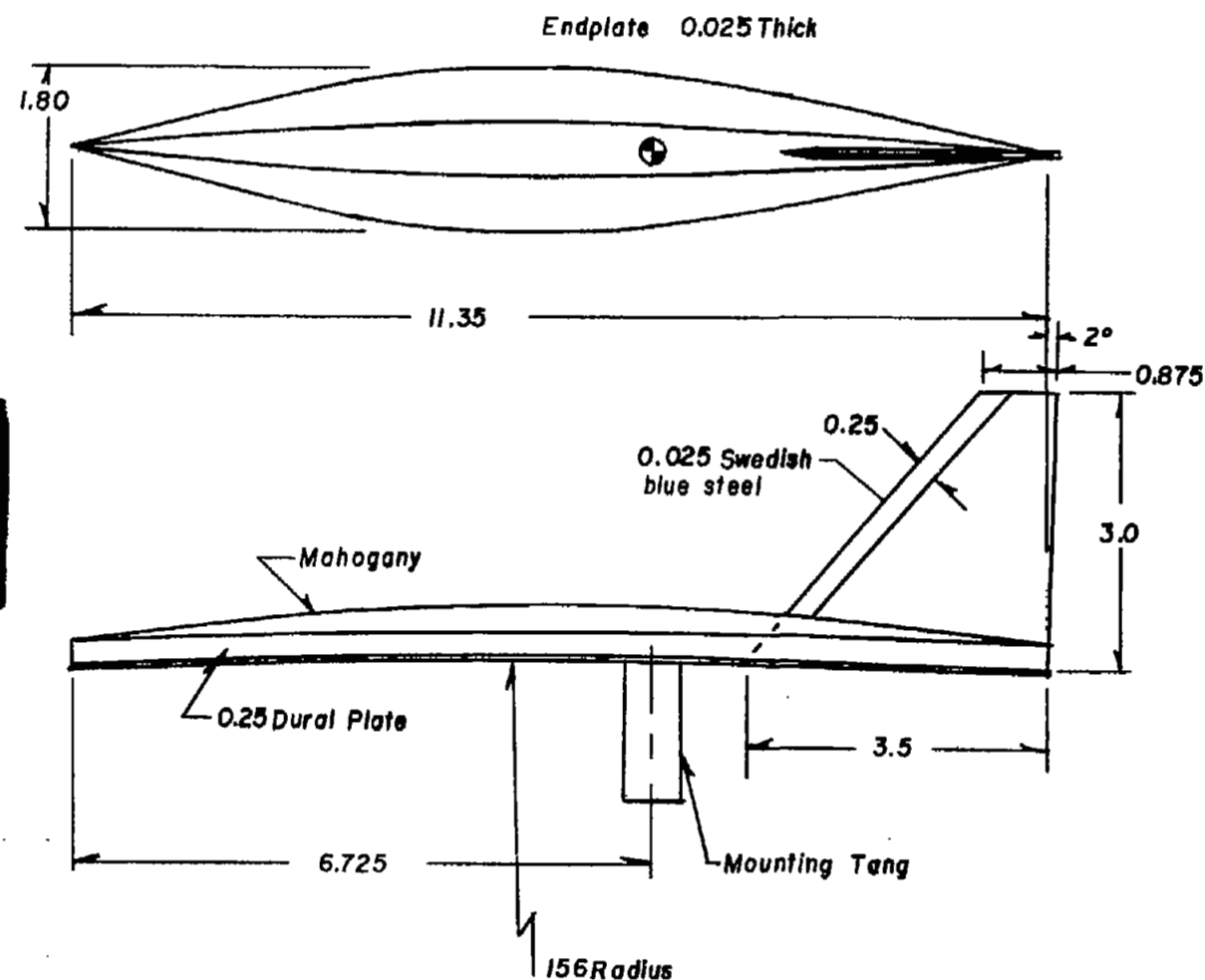
BODY COORDINATES
PERCENT LENGTH

STA	BASIC FUSELAGE RADIUS
0	0
11.892	0.925
20.705	1.804
29.515	2.185
38.326	2.511
47.137	2.643
55.947	2.555
64.758	2.222
73.568	1.709
82.379	1.137
91.189	0.513
100	0

Basic Fuselage Radius

Typical Crossection

NACA

Figure 6.- Drawing of second model.   Dimensions are in inches.
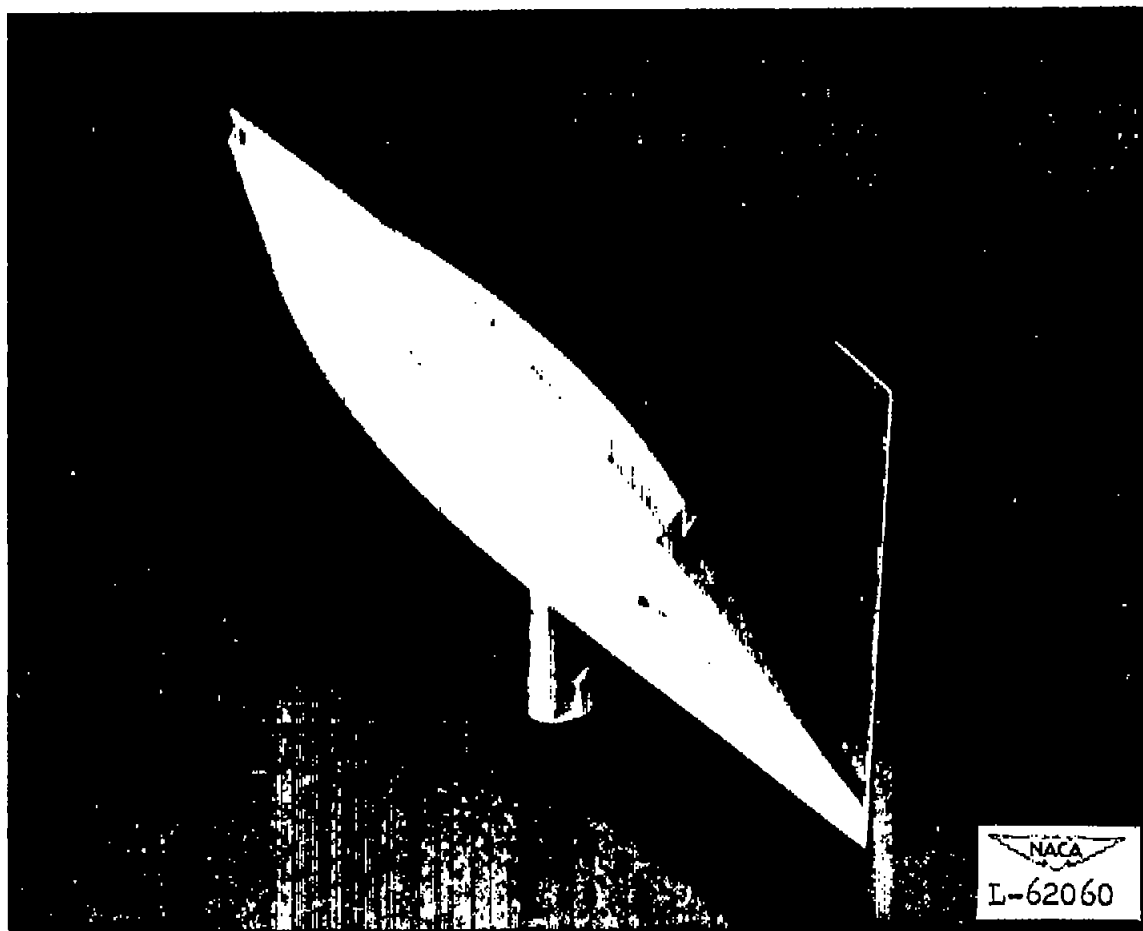
Figure 7.- Photograph of second model.
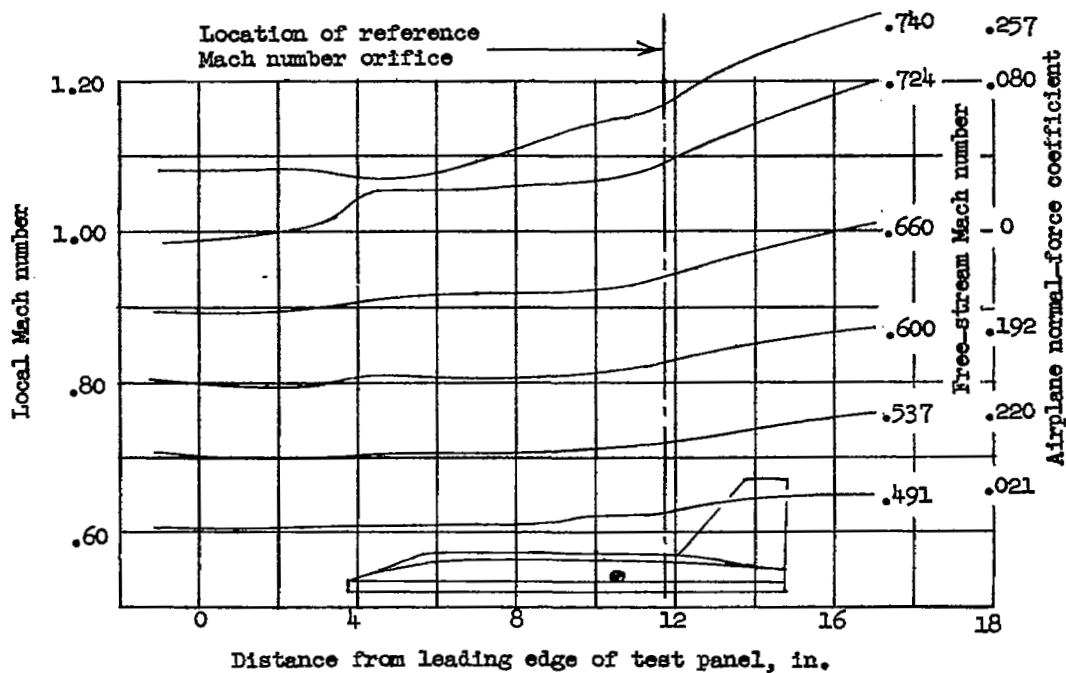
(a) Local Mach number distribution.
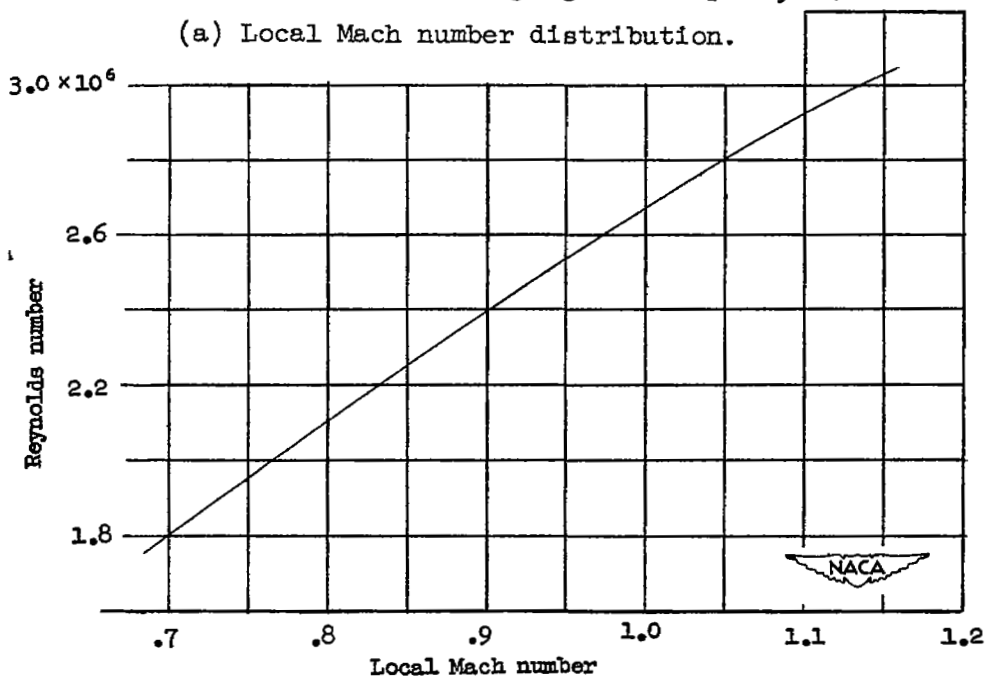
(b) Reynolds number against Mach number.

Figure 8.- Local Mach number distribution near surface of wing-flow test
    panel and variation of Reynolds number (based on body length) with
    Mach number.
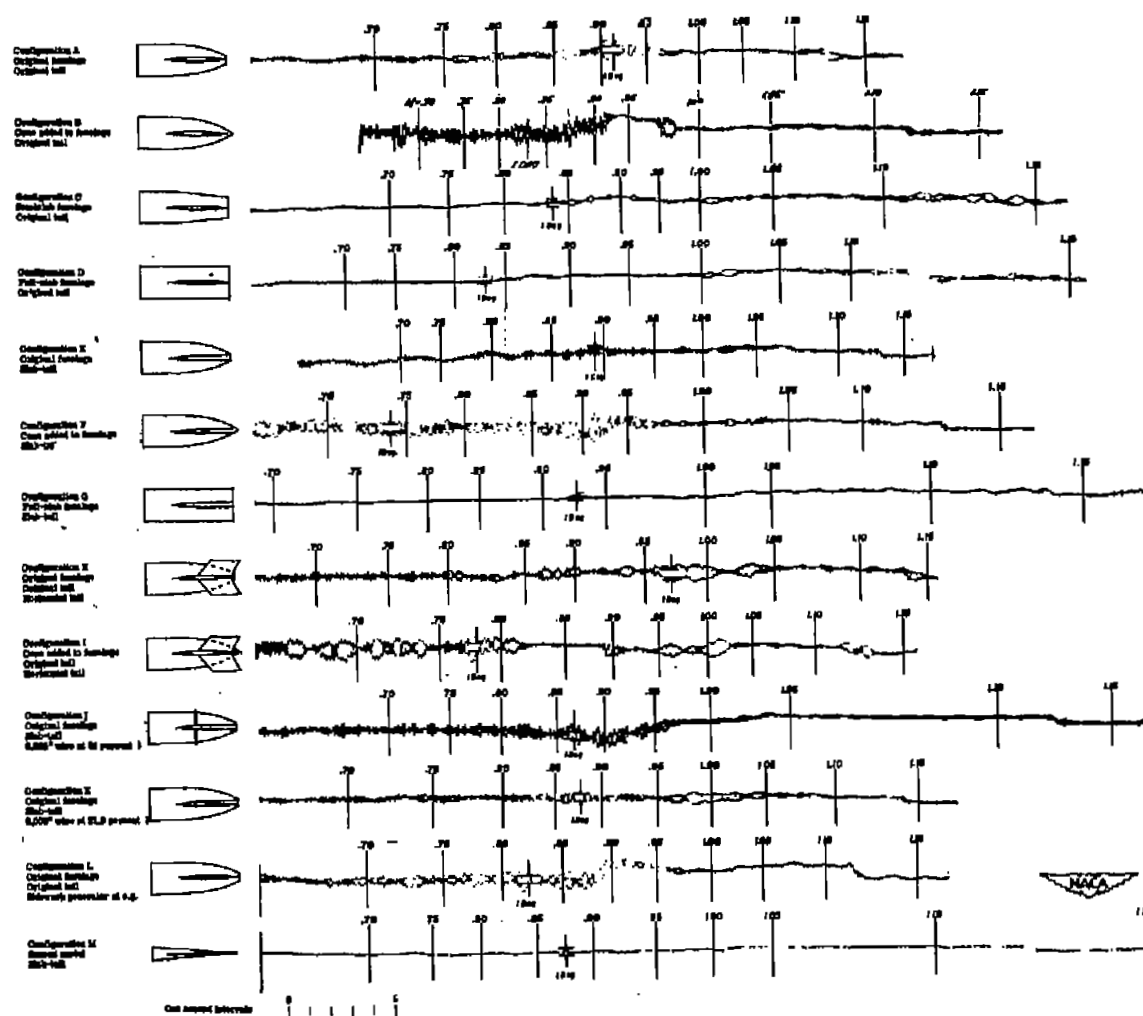
Figure 9.- Records of directional oscillation characteristics of all model configurations investigated throughout Mach number range tested. (A 17 by 22 inch print of this figure appears in the back of this report.)

Figure 10.- Tuft photograph taken at a Mach number of 0.86. Note blurring of two rearmost body tufts.
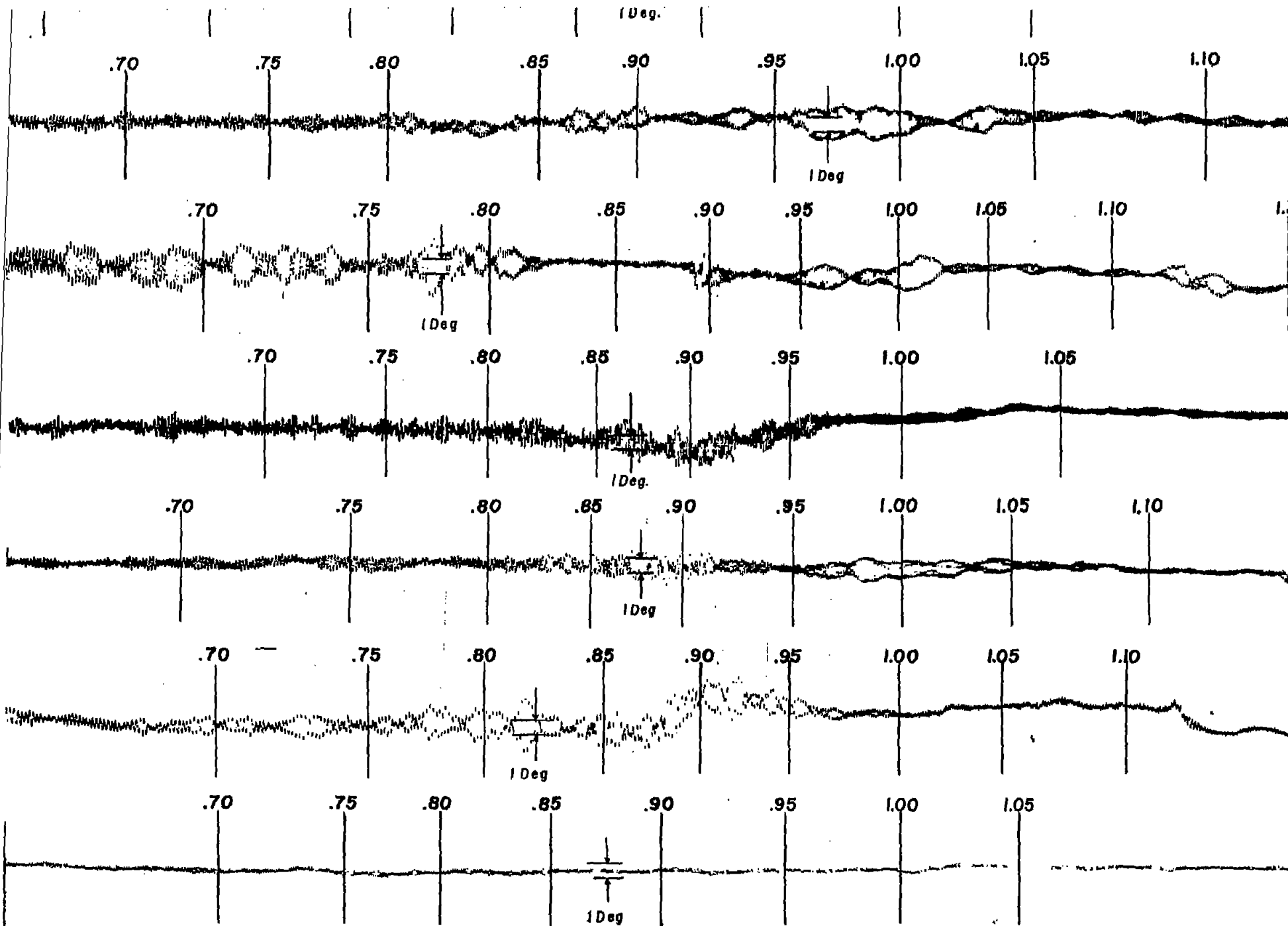
Figure 9.- Records of directional oscillation characteristics of all
model configurations investigated throughout Mach number range tested.

Configuration A
Original fuselage
Original tail

.70   .75   .80   .85
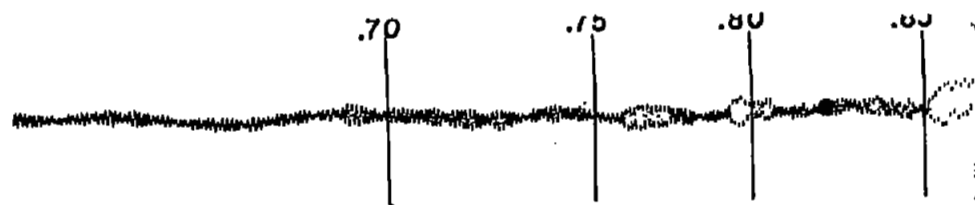
Configuration B
Cone added to fuselage
Original tail

$M=.70$ .75   .80   .85
I DEG
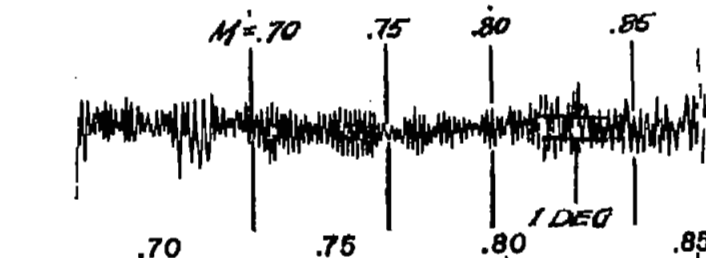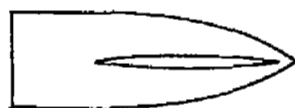
Configuration C
Semislab fuselage
Original tail

.70   .75   .80   .85
I Deg
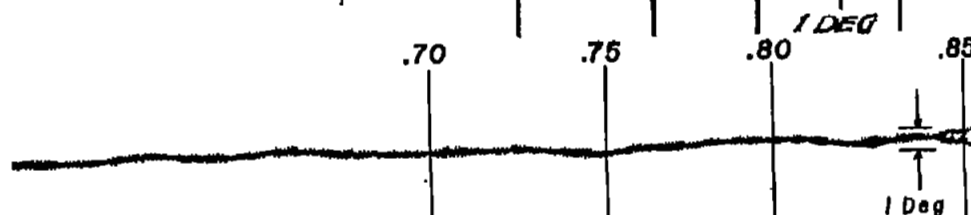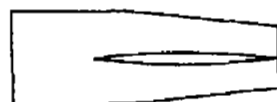
Configuration D
Full-slab fuselage
Original tail

.70   .75   .80   .85   .90
I Deg
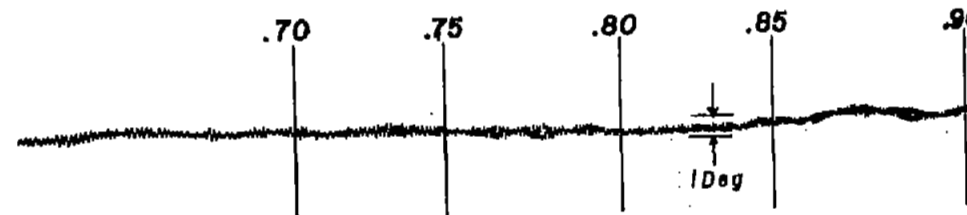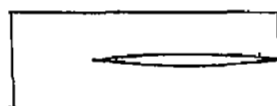
Configuration E
Original fuselage
Slab-tail

.70   .75   .80   .85
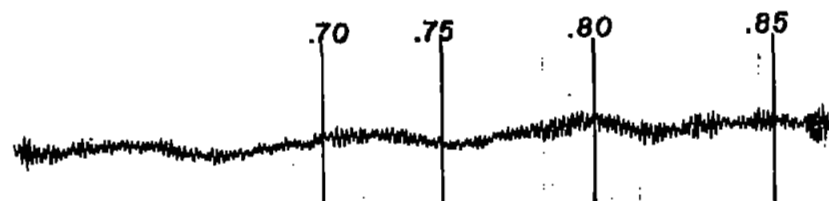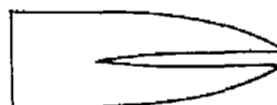
Configuration F
Cone added to fuselage
Slab-tail

.70   .75   .80   .85
I Deg.
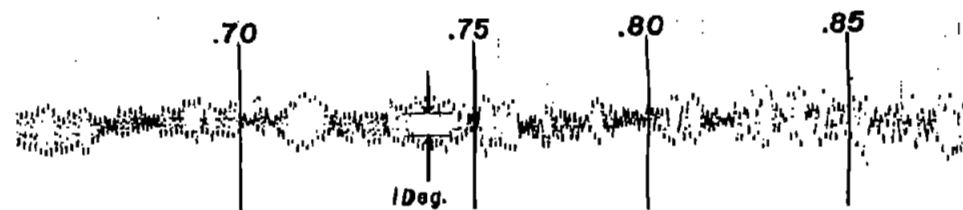
Configuration G
Full-slab fuselage
Slab-tail

.70   .75   .80   .85   .90
I De

90   .95   1.00   1.05   1.10   1.15

1 Deg

90   .95   1.00   1.05   1.10   1.15

.90   .95   1.00   1.05   1.10   1.15

.95   1.00   1.05   1.10   1.15

.90   .95   1.00   1.05   1.10   1.15

Deg

.95   1.00   1.05   1.10   1.15
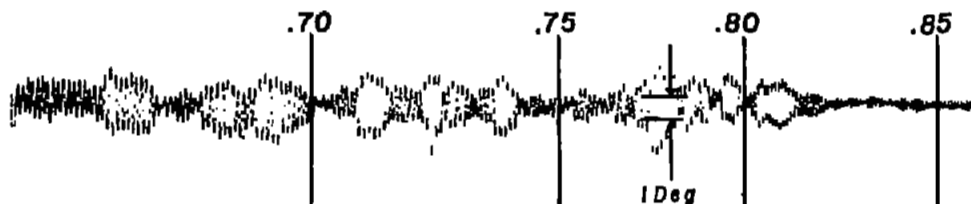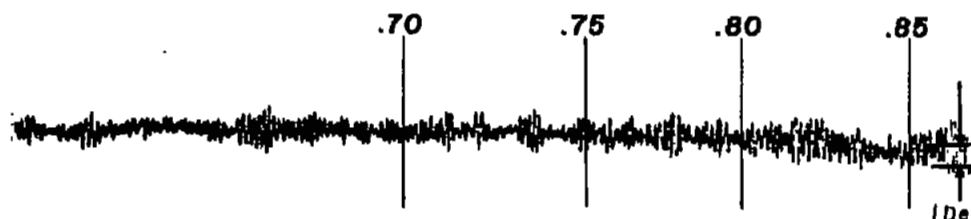
.95   1.00   1.05   1.10   1.15
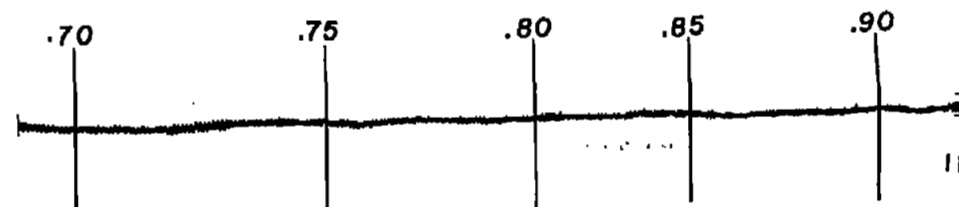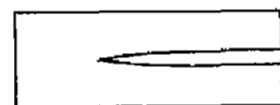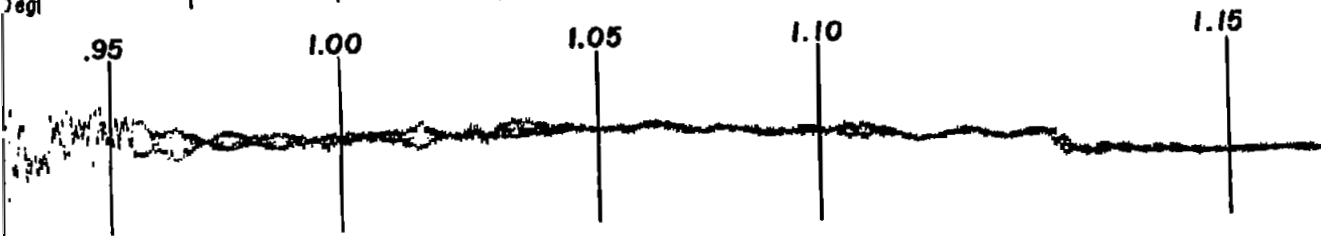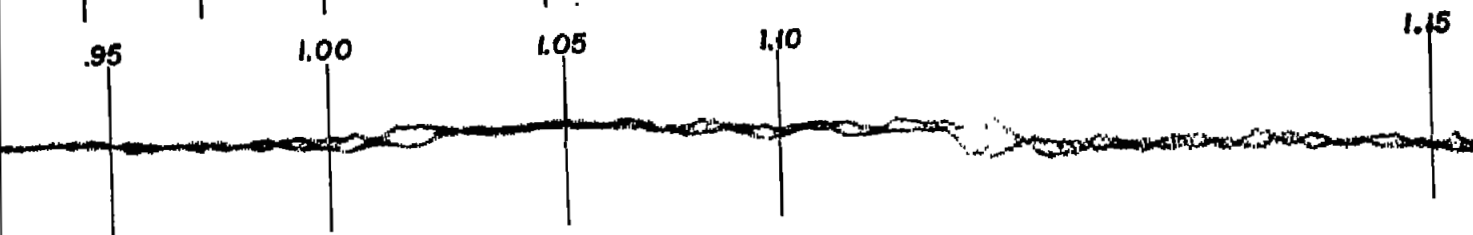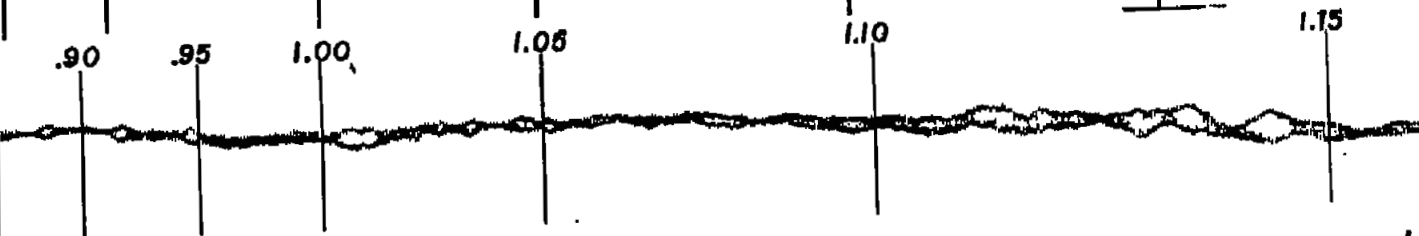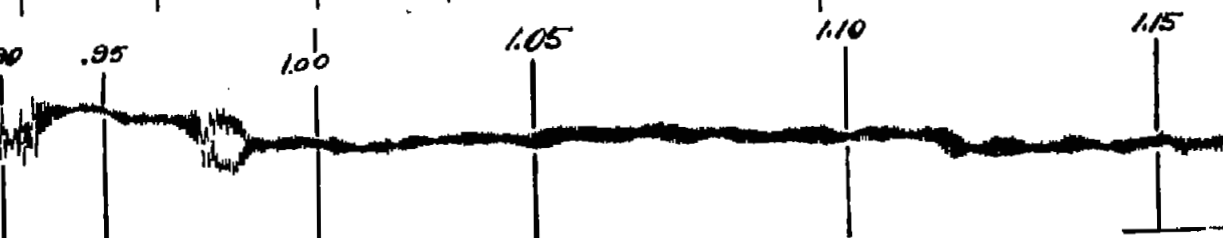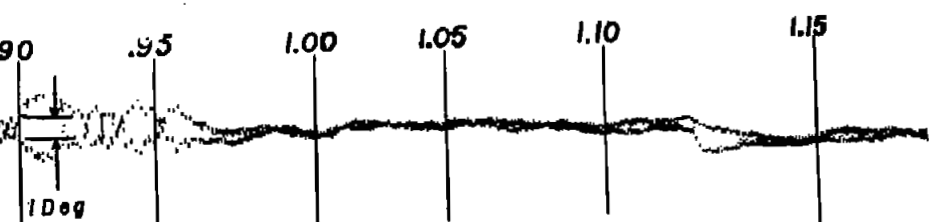
Configuration H
Original fuselage
Original tail
Horizontal tail

.70   .75   .80   .85   .9

Configuration I
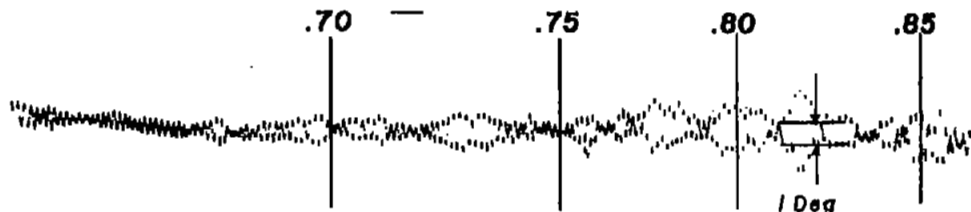Cone added to fuselage
Original tail
Horizontal tail

.70   .75   .80   .85

1 Deg

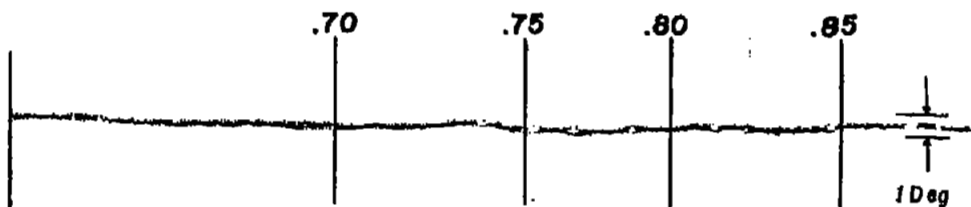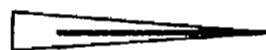Configuration J
Original fuselage
Slab-tail
0.065" wire at 84 percent l

.70   .75   .80   .85

1 De

Configuration K
Original fuselage
Slab-tail
0.005" wire at 21.9 percent l

.70   .75   .80   .85

1 D
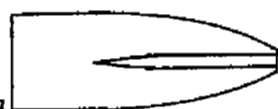
Configuration L
Original fuselage
Original tail
Sidewash generator at c.g.

.70   .75   .80   .85

1 Deg

Configuration M
Second model
Slab-tail

.70   .75   .80   .85

1 Deg

One second intervals

0   5

Figure 9.- Records of direc-
model configurations inve

.95 1.00 1.05 1.10 1.15

I Deg

.90 .95 1.00 1.05 1.10 1.15

.90 .95 1.00 1.05 1.10 1.15

.90 .95 1.00 1.05 1.10 1.15

.90 .95 1.00 1.05 1.10 1.15

NACA

0 .95 1.00 1.05 1.10 1.15

hal oscillation characteristics of all
igated throughout Mach number range tested.